Bioorganic & Medicinal Chemistry Letters 24 (2014) 1315–1321

Contents lists available at ScienceDirect

Bioorganic & Medicinal Chemistry Letters

journal homepage: www.elsevier.com/locate/bmcl

HTS followed by NMR based counterscreening. Discovery and optimization of pyrimidones as reversible and competitive inhibitors of xanthine oxidase

Johan Evenäs [b,†], Fredrik Edfeldt [c], Matti Lepistö [a], Naila Svitacheva [b], Anna Synnergren [b], Britta Lundquist [b], Mia Gränse [b], Anna Rönnholm [b], Mikael Varga [a], John Wright [d], Min Wei [d], Sherrie Yue [d], Junfeng Wang [d], Chong Li [d], Xuan Li [d], Gang Chen [d], Yong Liao [d], Gang Lv [c], Ann Tjörnebo [b], Frank Narjes [a,*]

[a] Department of Medicinal Chemistry, Respiratory Inflammation and Autoimmunity Innovative Medicines, AstraZeneca R&D, Pepparedsleden 1, SE-431 83 Mölndal, Sweden
[b] AstraZeneca R&D Lund, Scheelevägen 1, SE-221 87 Lund, Sweden
[c] Discovery Science, AstraZeneca R&D, Pepparedsleden 1, SE-431 83 Mölndal, Sweden
[d] Department of Medicinal Chemistry, DMPK and Biology, BioDuro, Life Science Park Road Bld 2, Beijing 102206, PR China

ARTICLE INFO

Article history:
Received 25 November 2013
Revised 18 January 2014
Accepted 20 January 2014
Available online 28 January 2014

Keywords:
Xanthine oxidase
High-throughput screening
Hit-to-lead
Non-purine XO inhibitors
Pyrimidone

ABSTRACT

The identification of novel, non-purine based inhibitors of xanthine oxidase is described. After a high-throughput screening campaign, an NMR based counterscreen was used to distinguish actives, which interact with XO in a reversible manner, from assay artefacts. This approach identified pyrimidone **1** as a reversible and competitive inhibitor with good lead-like properties. A hit to lead campaign gave compound **41**, a nanomolar inhibitor of hXO with efficacy in the hyperuricemic rat model after oral dosing.

Mammalian xanthine oxidoreductase (XOR) catalyzes the last two steps of purine catabolism in man, namely the oxidation of hypoxanthine to xanthine and further to uric acid. The enzyme is initially synthesized as xanthine dehydrogenase (XDH), but in mammals it can be easily converted to xanthine oxidase (XO).[1] The latter uses molecular oxygen as the electron acceptor during purine oxidation, generating reactive oxygen species (ROS). XO-derived ROS has been implicated in a number of disease states such as inflammation, metabolic disorders, atherosclerosis, carcenogenesis and chronic obstructive pulmonary disease (COPD).[2–5]

Currently there are no registered therapies available to treat oxidative stress in COPD patients, but inhibitors of XO are used clinically for the treatment of gout, with allopurinol, a mechanism-based inhibitor, being the first-line therapy.[2] Several side-effects such as skin rashes, gastrointestinal problems, drowsiness and hypersensitivity have been reported for allopurinol, potentially due to toxic purine metabolites.[2,6] These limitations have prompted the search for non-purine based XO inhibitors.[1,2] Examples include the recently approved Febuxostat,[7] the related piraxostat[8] or FYX-051.[9] Other structural classes reported in the recent literature are isocytosines,[10] thiadiazolo-pyrimidones,[11] Schiff bases of benzaldehydes,[12] xanthones,[13] and *N*-(1,3-diaryl-3-oxopropyl)amides (Fig. 1).[14]

To find novel, reversible inhibitors of XO for the treatment of oxidative stress in COPD, we conducted a high-throughput screening (HTS) campaign of the AstraZeneca corporate compound

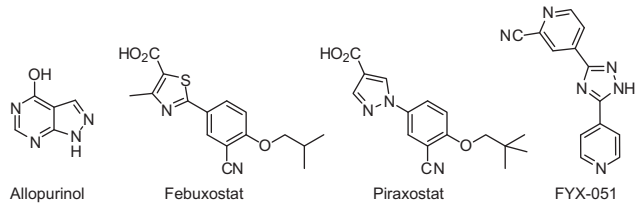

Figure 1. Reported XO inhibitors.

* Corresponding author. Tel.: +46 31 706 46 64; fax: +46 31 776 37 92.
E-mail addresses: johan.evenas@redglead.com (J. Evenäs), Frank.Narjes@astrazeneca.com (F. Narjes).
† Current address: Red Glead Discovery, Scheelevägen 17, 22370 Lund, Sweden.

http://dx.doi.org/10.1016/j.bmcl.2014.01.050
0960-894X/

collection using bovine XO and colorimetric detection of uric acid formation as the readout.[15] Around 2500 compounds with an IC_{50} <10 μM were identified, which were clustered according to 2D fingerprints and Tanimoto index. After removal of unwanted chemotypes, selected cluster representatives and singletons were tested in a further optimized assay on bovine and human XO. Both assays correlated well with each other and confirmed the results obtained from the HTS assay. To distinguish reversible inhibitors from false positives such as assay artefacts or compounds with an undesired mechanism of inhibition such as suicide inhibitors, we established a novel NMR-based binding assay for XO as an orthogonal read-out to the biochemical assay.[16] Ligand-observed 1D ^{1}H T1rho experiments of HTS actives were recorded in the absence and presence of bXO. An intensity reduction upon addition of protein is indicative of compound binding. After addition of a high affinity ligand such as Febuxostat, any observed displacement (i.e. re-gained intensity) of the compound would be indicative of reversible and competitive binding.[17] Validation of the method using XO inhibitors with an established mechanism of inhibition is shown in Figure 2. The proton NMR signals of allopurinol at 8.30 and 8.15 ppm were reduced in intensity upon addition of bXO, indicative of binding (Fig. 2a). A singlet at 8.1 ppm appeared, belonging to oxopurinol, which is released from the enzyme, upon conversion of Mo(IV) back to Mo(VI).[6] A reduction in signal intensity was also observed for salicylate, a reversible, low affinity inhibitor (K_i = 100 mM).[18] This could be reversed by addition of Febuxostat, whose aromatic protons appear at 7.3, 8.1 and 8.2 ppm (labeled with asterisks, Fig. 2b).

Figure 2c shows the case for the suicide inhibitor FYX-051. The reduction in ligand signals observed after addition of bXO cannot be reversed by addition of Febuxostat. Different from allopurinol, no new peaks appeared over time, since the oxidized form of FYX-051 remained covalently bound to the enzyme.[9]

Figures 2d–f illustrate the use of the NMR assay in the profiling of compounds **1**–**3** as representative members of our HTS output. Arylpyrimidine **1** clearly behaved as a competitive, reversible binder (Fig. 2d). Triazolo-thiadiazole **2** (Fig. 2e) showed a behavior reminiscent of a potential suicide inhibitor, since signal intensity was not regained upon addition of Febuxostat. Phenylpteridine **3** (Fig. 2f) was oxidized, as evidenced by the disappearance of the signal at 8.4 ppm and the shift of the peak at 8.2 ppm to 8.0 ppm. Imidazo-pyrimidin-one **4** had all the characteristics of a reversible binder, whereas the closely related imidazo-triazine **5** was oxidized analogously to allopurinol (spectra not shown). These experiments demonstrate that NMR can be used to study binding to XO and that it can distinguish competitive reversible inhibitors from

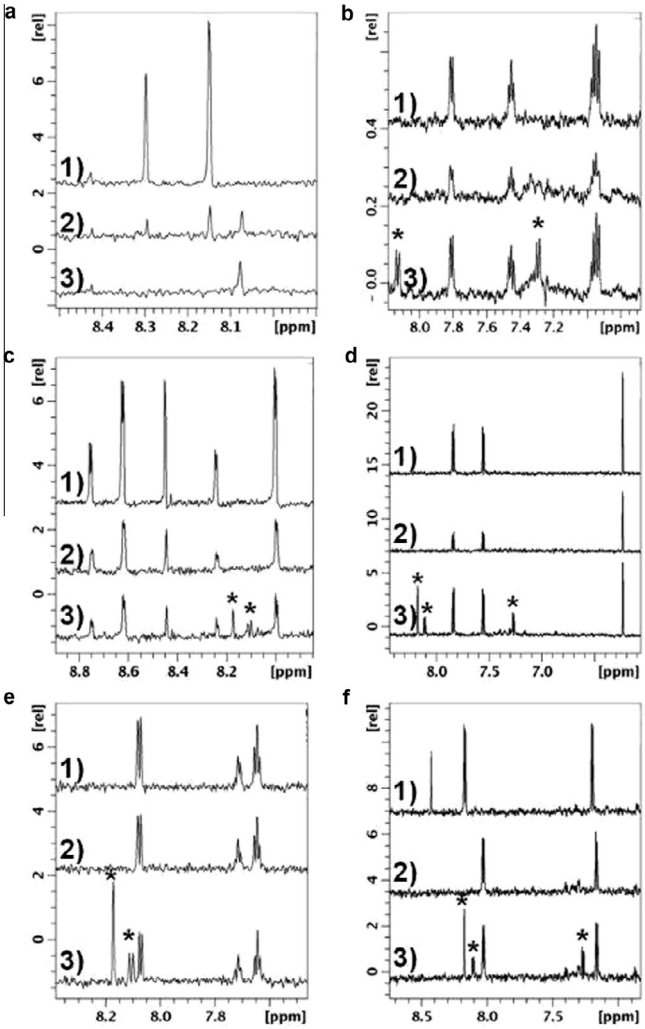

Figure 2. 1D $T_{1\rho}$ ^{1}H NMR spectra of XO inhibitors and HTS hits: Spectrum 1): compounds only at ~50 μM in buffer; spectrum 2) 2 μM bXO added; spectrum 3) addition of 30 μM Febuxostat (aromatic H labeled with asterisk); (a) allopurinol (no Febuxostat added in experiment 3); (b) salicylate; (c) FYX051; (d) compound **1**; (e) compound **2**; (f) compound **3**.

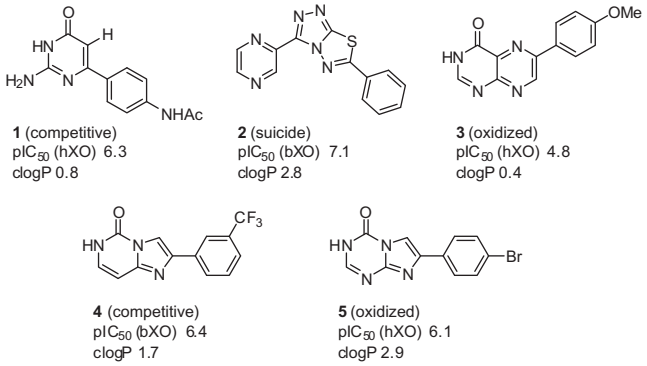

Figure 3. HTS hits.

Table 1

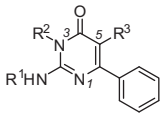

Compound	R1	R^2	R^3	hXO[a] pIC_{50}	pK_a[b] B1/A (calcd)	LLE[c]
6	H	H	H	4.8	−/9.2 (2.6/9.2)	3.5
7	Me	H	H	5.1		3.3
8	Bn	H	H	4.8		1.3
9	Ac	H	H	<4.0		–
10	$MeSO_2$	H	H	<4.0		–
11	H	Me	H	<4.0		–
12	H	H	F	4.9	2.2/7.6 (1.7/7.3)	3.4
13	H	H	Cl	6.1	2.4/7.45 (1.2/7.4)	3.9
14	H	H	Br	6.0	– (1.2/7.4)	3.7
15	H	H	CN	6.1	0/6.5 (−/6.8	4.1
16	H	H	Me	4.6	4.4/9.6 (3.2/9.3)	2.9
17	H	H	Ph	5.9	3.8/9.2 (2.6/9.2)	3.4

[a] Values are the mean of at least two independent experiments.
[b] Measured pK_a of the 2-amino (B1) and *N*3-NH (A1). In brackets values calculated using ACD-Lab 12.3.
[c] Lipophilic ligand efficiency: $pIC_{50}-c\log P$.[19]

less desirable mechanisms or assay artefacts. This method can also be used for a fragment-based screening approach, since it detected binding of low affinity inhibitors such as salicylate. The NMR assay was preferred over kinetic measurements, as it provided more direct information on the binding mechanism by monitoring the ligand at atomic resolution and also due to its efficient implementation. Overall, only five clusters and one singleton showed unambiguous reversible binding behavior without any oxidation of the compounds (Fig. 3).

Pyrimidone **1** presented an attractive starting point due to its potency and high lipophilic ligand efficiency (LLE = 5.5).[19] It also showed good solubility from amorphous material, had low intrinsic clearance in human hepatocytes (2.7 mL/mg/10^6 cells) and did not inhibit major P450 cytochromes.[20]

During the course of this work, Rao et al. reported the identification of similar 4-arylpyrimidones as XO inhibitors from a virtual screening approach.[10a] Optimization of their hit led to compounds such as **18** (Table 2).[10b] Further improvements towards an orally efficacious inhibitor were realized mainly by modifications of the isobutyl ether on the aryl ring and removal of substituents in the 2- and 4-position of the pyrimidone.[10c] Our own hit-to-lead effort around **1** focused on the pyrimidone core and the 4-aryl group itself. We monitored LLE during the optimization of **1** and chose modifications which resulted in enhancement of both potency and LLE.[19] This effort identified a lead series of very potent 5-substituted pyrimidone inhibitors of human XO, which demonstrated efficacy in the rat model of hyperuricemia after oral dosing.

Table 2

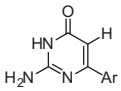

Compound	Ar	hXO[a] pIC_{50}	Sol[b] (μM)	HLM[c] Cl_{int}	LLE[d]
6		4.8			3.5
18	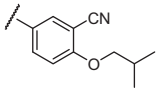	7.6	140	7.9	4.8
19	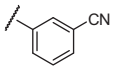	6.1		–	5.2
20	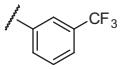	6.2	36		4.5
21	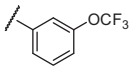	6.7	330	3.2	4.5
22		5.0		–	3.1
23	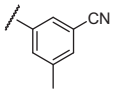	7.0	350	1.2	5.5
24	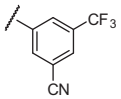	6.1	430	0.2	4.8
25	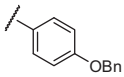	6.1	<1	–	3.5
26	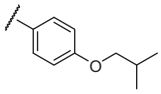	6.3	23	42	3.6
27	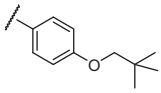	6.7	3.1	6.9	3.6
28	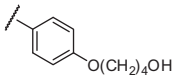	6.0	95	6.8	4.9
29	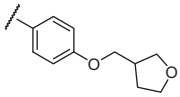	6.3	58	21	4.9
Febuxostat	–	8.9	–	–	–

[a] Values are the mean of at least three independent experiments.
[b] Solubility determined at pH 7.4 (phosphate buffer).
[c] Human liver microsome intrinsic clearance (μL/min/mg).[23]
[d] Lipophilic ligand efficiency: $pIC_{50}-c\log P$.[19]

The initial SAR around **1** is summarized in Table 1. Removal of the aminoacetyl group from **1** led to **6** showing a 20-fold drop in potency. Only methyl substitution was accepted on the exocyclic amino group of **6** (**7**, pIC_{50} = 5.1), whereas other residues had no effect (see **8**), or were detrimental (compounds **9** and **10**). Methylation of *N*-3 yielded inactive **11**, pointing to a critical role for that group. Introduction of a substituent in the 5-position, such as chloro (**13**) or bromo (**14**), or a nitrile (**15**) led to a more than 10-fold gain in potency. Interestingly, a fluorine was not effective (**12**, pIC_{50} = 4.9). A methyl group was slightly worse than hydrogen, whereas the introduction of a phenyl group had an effect similar to halogen. Overall, the only modification of **6**, which led to a significant increase in potency and LLE was achieved by the introduction of Cl and CN in the 5-position.

Based on these initial results, we docked compound **13** into a homology model of hXO constructed from the X-ray crystal structure of bXO in complex with Pyraxostat and Febuxostat (Fig. 4).[21] According to this model, **13** blocks access to the catalytic center similar to Febuxostat, and their ring systems overlap significantly. Compound **13** establishes several hydrogen bond and hydrophobic interactions. The amino group in the 2-position of the pyrimidone ring donates H-bonds to one of the Mo-Pt-oxido(−1) oxygens and Glu802. There appears to be room for a substituent no larger than methyl (R^1 in Table 1), explaining the drop in activity for compounds **9** and **10**. These substituents would clash with E1261. The *N*-3 and the carbonyl (or hydroxyl enol) mimics the carboxyl group of Febuxostat and maintains H-bonding interactions with Arg880 and Thr1010 in similar manner. It is also stacked between Phe914 and Phe1009 (not shown). Methylation of *N*-3 would be expected to be detrimental for these interactions, as was observed for compound **11**. Substituents in the 5-position point towards a sub-pocket, which is formed by the interdomain loop (id-loop) containing Thr1010 and Val1011. It is large enough to accommodate halogens and groups of similar size such as methyl or cyano. Electronegative substituents in the 5-position lower the pK_a of the hydrogen-bond donors on the pyrimidone (Table 1) and this is expected to strengthen the hydrogen bond network and thus increase potency.[22] This could account for the different effect of a chloro or cyano versus a methyl group on potency. Fluorine would not fill the sub-pocket, maybe explaining why despite the observed lowering of the pK_a of the hydrogen bond donors, a gain in potency was not observed. To accommodate the larger phenyl residue would require movement of the id-loop (see Supplementary material).

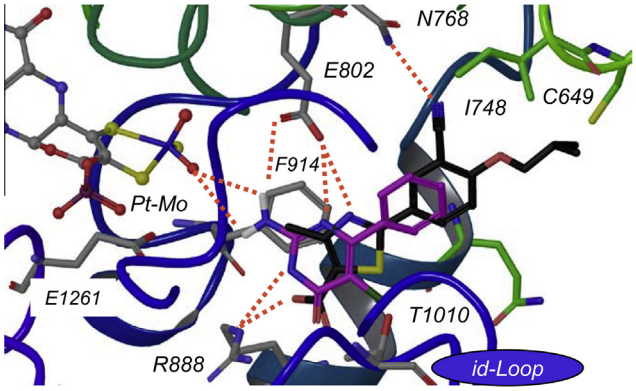

Figure 4. Febuxostat (black carbons) and compound **13** (magenta carbons) docked into a homology model of human XO (Prime/Maestro, Schrodinger Inc.). Protein residues are displayed in green when they are different from bXO, otherwise in grey. The loop connecting the 2-layer sandwich domains is denoted 'id-Loop'. Further details on model building, coordinates and an additional view can be found in the Supplementary material.

A similar binding mode, with overlap between the pyrimidone and Febuxostat, was also proposed by the Rao group.[10a]

The overlay of **13** with Febuxostat suggested applying the substitution pattern of the phenyl ring to the pyrimidone series, hoping it would pick up the interaction between the 3-cyano group and Asn768 and the hydrophobic contacts of the 4-isobutoxy tail. Compound **18**, boosting the potency of **6** by nearly 3 orders of magnitude, confirmed this assumption (Table 2). In the NMR assay **18** showed reversible and competitive binding versus Febuxostat. Further SAR on the aromatic ring revealed that *ortho*-substitution, which would disturb the nearly coplanar arrangement of the phenyl and the pyrimidone ring, was not tolerated (data not shown). Substitution in the *meta*-position with a cyano, trifluoromethyl or a trifluoromethoxy group enhanced potency and also LLE significantly (compounds **19**–**21**). A simple methyl group (**22**) was not significantly better than **6**, but the combination with the 3-cyano substituent further enhanced potency and LLE with respect to **19** (**23**, pIC_{50} = 7.0, LLE = 5.5). The combination of two electron-withdrawing groups such CF_3 and CN (**24**, pIC_{50} = 6.1) did not provide any advantage. In the *para*-position a variety of substituents such as esters, acetamides or reversed acetamides were tolerated or led to some potency gain. Eventually, we settled on the ether moiety. Relatively simple residues such as benzyl, isobutyl or neopentyl led to a more than 10-fold boost in potency, but not to an increase in LLE. As a consequence of the higher lipophilicity, compounds **25**–**27** showed rather low solubility. Addition of a solubilizing group such as an alcohol (**28**) or a tetrahydrofuryl moiety (**29**) not only increased solubility, but also maintained potency with an increase in LLE with respect to **26**. Most of the compounds showed good stability in human liver microsome preparations, with the exception of **26** and **29**, which had higher intrinsic clearance.

The final round of SAR combined the most ligand-efficient residues identified previously (Table 3). Addition of the nitrile or chloro-substituent in the 5-position of **18** led to a more than 10-fold increase in potency. Nitrile **30** inhibited hXO with subnanomolar potency, whereas the chloro analogue **31** was about 3-fold less potent. Different from the simpler analogue **7**, N-methylation was not tolerated and resulted in a 100-fold loss in potency (**32**, pIC_{50} = 6.3). Due to the overall good profile with respect to solubility and metabolic stability, **30** was dosed to Han-Wistar rats in preparation for the hyperuricemic rat model.[24] Low plasma clearance and long half-life were observed after intravenous dosing, but oral bioavailability was low. Testing in the Caco2 assay revealed low permeability and high efflux for **30**, whereas the chloro analogue **31** showed improved permeability and a lower efflux ratio.[25] Alcohol **33** showed better solubility than **31**, with only a 2-fold loss in potency, but permeability and efflux were not improved. To obtain an optimal balance of the desired properties, changes to the aryl substitution pattern were investigated in the cyano and the chloro series. Compounds **34** and **35** were found to be potent, soluble and stable, but demonstrated the same low permeability and high efflux, whereas compound **36** was rather poorly active. An exception was **37**, which showed improved permeability and efflux ratio with respect to **31**. An analysis of the SAR obtained so far indicated that 5-unsubstituted and 5-chloro substituted pyrimidones were superior to 5-cyano compounds with respect to permeability, and that the polar surface area (PSA) should ideally be below 100 $Å^2$ (Table 3). Our efforts in the 5-chloro subseries confirmed this, where compounds such as **38** with a PSA of 107 $Å^2$ had low permeability, but analogs **39**–**41** demonstrated enhanced permeability, although significant efflux was still observed. Based on their overall profile, compounds **40** and **41** were dosed to rats and displayed improved oral bioavailability compared to **31**. As Table 3 shows, combination of the most ligand-efficient residues resulted on the whole in a further gain in

Table 3

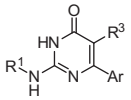

Compound	R^1	Ar	R^3	hXO[a] pIC_{50}/LLE[b]	Sol[c] (μM)	HLM[d] Cl_{int}	Caco2[e]		PSA[f] (Å^2)	Rat PK[g] iv: Cl (mL/min/kg), $t_{1/2}$ (h) po: V_{ss} (L/kg), C_{max} (μM), F
							P_{app}	Efflux ratio		
30	H	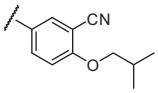	CN	9.3/5.8	14	4.1	0.1/30	300	117	1.8; 19.0 2.5; 0.07, 5.5%
31	H	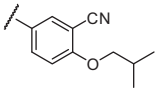	Cl	8.8/5.1	3.1	16	5.7/65	11.4	98	–
32	Me	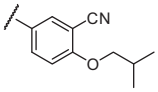	CN	6.3/2.4	37	3.6	–	–	–	–
33		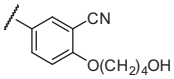	Cl	8.4/6.3	93	1.7	0.2/25.6	128	121	–
34		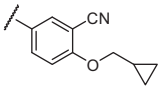	CN	8.9/6.0	45	1.7	0.1/31	310	117	–
35		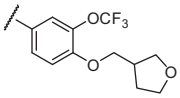	CN	9.2/6.7	86	21	0.1/29	290	116	–
36		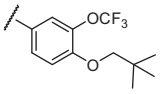	CN	7.7/3.5	6	36	0.4/4.1	10	107	–
37		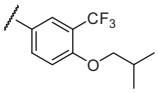	CN	8.9/5.2	1.2	8.5	1.7/23	13.5	98	–
38		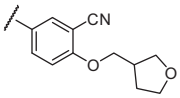	Cl	8.8/6.4	41	3.4	0.2/24	120	107	–
39		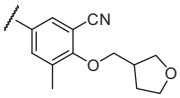	Cl	8.2/5.3	83	5.3	2.1/35	17	107	–
40		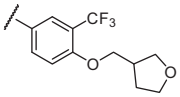	Cl	8.2/5.6	24	7.5	8.4/69	8.2	88	15; 10.0 5.7; 0.27, 33%
41		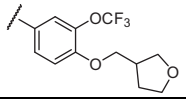	Cl	9.0 / 6.2	45	18	6.4 / 74	11.5	97	35; 13.2 13; 0.08, 22%

[a] Values are the mean of at least three independent experiments.
[b] lipophilic ligand efficiency: pIC_{50}—$c\log P$.[19]
[c] Determined at pH 7.4 from DMSO stock solutions.
[d] Human liver microsome intrinsic clearance (μL/min/mg).[23]
[e] Caco2: A to B/B to A, (10^{-6} cm/s).[25]
[f] Polar surface area, calculated using ACD-Lab.
[g] Compounds **30, 40** and **41** were dosed to male Han Wistar rats, $n = 3$; iv, 1 μmol/kg, solution in TEG/water (50:50); po 6 μmol/kg, suspension in 0.5% HPMC.

LLE with respect to **18**. A series of potent, soluble and stable compounds, exemplified by **30**, **33**–**35**, and **38-41**, could be obtained. In the NMR assay, compounds **30**, **35**, **38** and **40** showed reversible and competitive binding versus Febuxostat.

The effect of compound **41** on serum uric acid levels was evaluated in hyperuricemic rats.[24,26] Its potency on rat XO was determined to be 10-fold lower than on hXO (pIC_{50} rat = 8.1), similar to Febuxostat (pIC_{50} rat = 8.4). One hour after induction of hyperuricemia to overnight fasted rats, compound **41**, allopurinol or Febuxostat were administered orally at the indicated doses. Animals treated with **41** at an oral dose of 10 mg/kg had about 54% lower serum uric acid levels than the vehicle control group at 2 h (1 h, 55% reduction), but was not as effective as allopurinol at 30 mg/kg or Febuxostat at 10 mg/kg, which showed reductions of 94% (1 h, 87%) and 75% (1 h, 78%) respectively (Fig. 5). Plasma levels of compound **41** at 2 h were about 22-fold lower (0.37 ± 0.1 μM) than those for Febuxostat (8.7 ± 3.5 μM), explaining the difference in uric acid levels.

In summary, we have shown that an NMR-based counterscreen as an orthogonal assay aided in the selection of high quality leads

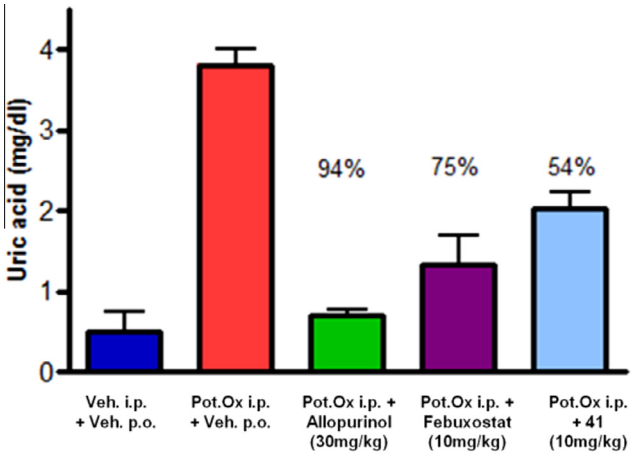

Figure 5. Antihyperuricemic effect of allopurinol, Febuxostat and **41** in hyperuricemic rats 2 h after oral dosing of compounds. Potassium oxonate was dosed to rats; a comparator group of rats received saline 1 h after potassium oxonate administration, and rats were dosed orally with vehicle, allopurinol (30 mg/kg), Febuxostat (10 mg/kg) or **41** (10 mg/kg).[26]

from our HTS output. A hit to lead campaign guided by LLE, identified inhibitors of hXO such as **30**. Further optimization with regard to permeability and solubility gave rise to single digit nanomolar inhibitors, which had suitable PK properties for evaluation in the hyperurecimic rat model. After an oral dose of 10 mg/kg, **41** lowered uric acid levels by 54%, thus providing a proof of concept for this series.

The synthesis of the 2-amino-6-aryl-pyrimidinones is exemplified in the following schemes. Compounds **6**–**11** were prepared according to literature methods.[27] Fluoro analog **12** was synthesized by fluorination of the methyl ketoester, followed by condensation with guanidine. Halogenation of **6** led to **13** or **14**,[27b] whereas nitrile **15** was prepared by condensation of benzaldehyde with ethyl 2-cyanoacetate and guanidine.[28] Suzuki coupling of **14** gave **17** (Scheme 1).[29]

Compounds from Table 2 were prepared either by reaction of appropriately substituted aryl-oxopropanoates with guanidine, or via Suzuki coupling of aryl boronic acids to 2-amino-6-iodo-pyrimidinone (see Supplementary material). Alkylation and borylation of appropriately substituted phenols **42** followed by formylation via halogen-metal exchange gave benzaldehydes **44**. Condensation with ethyl 2-cyanoacetate and guanidine led to cyanoderivatives **30** and **34**–**37**. For the *N*-methyl derivative **32**,

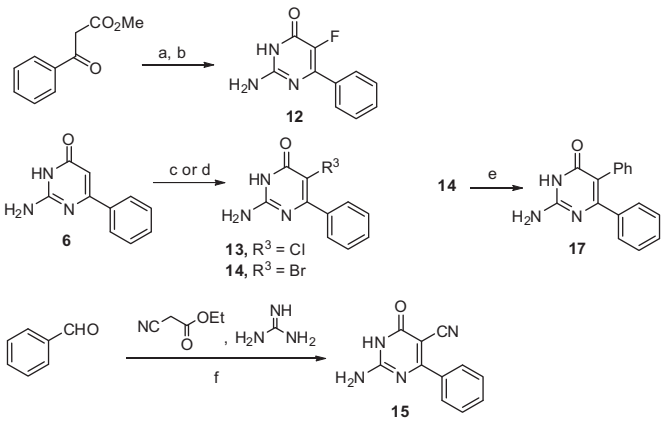

Scheme 1. Synthesis of 6-phenyl-pyrimidones. (a) Selectfluor™, CH_3CN, 80 °C, 5 h, 80%; (b) guanidine, EtOH, reflux, 12 h, 80%; (c) NCS, AcOH, 90 °C, 2 h, 48%; (d) NBS, AcOH, 90 °C, 2 h, 50%; (e) $Pd(PPh_3)_4$, Na_2CO_3, DMF, 80 °C, 24 h, 14%; (f) NaOAc, py, reflux, 4 h, 60%.

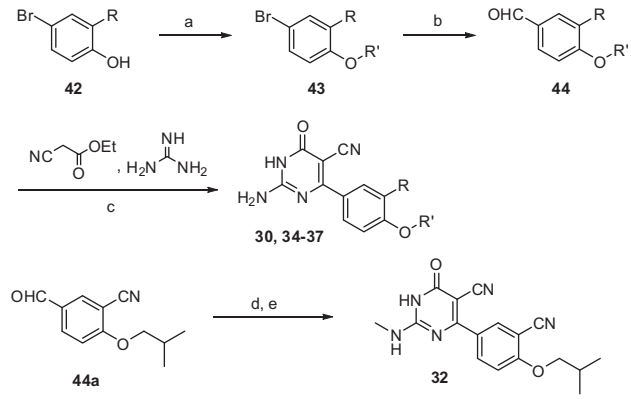

Scheme 2. Synthesis of 5-cyano pyrimidones. (a) R′-Br, K_2CO_3, DMF, 80 °C, 80–95%; (b) *n*-BuLi, THF, −78 °C, 20 min, then DMF, −78 °C to rt, 30–60%; (c) NaOAc, py, reflux, 4 h, 30–50%; (d) ethyl-2-cyanoacetate, thioguanidine carbonate, K_2CO_3, EtOH, reflux, 12 h, 40%; (e) $MeNH_2$, EtOH, microwave, 130 °C, 20 min, 25%.

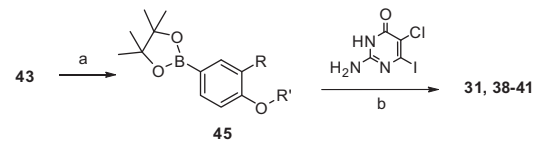

Scheme 3. Synthesis of 5-chloro pyrimidones. (a) $B_2(Pin)_2$, $Pd(dppf)Cl_2$, KOAc, DMSO, 80 °C, 12 h, 40–70%; (b) $Pd(dppf)Cl_2$, PCy_3, K_3PO_4, DMF, 100 °C, 12 h, 10–30%.

guanidine was replaced with thioguanidine in the condensation, and the thiogroup was substituted using methylamine (Scheme 2).

Chloro analogues **31, 33** and **38**–**41** were obtained from bromoethers **43** after their conversion to boronates **45** and coupling of the latter to 5-chloro-6-iodo-pyrimidone (Scheme 3).

Acknowledgments

The authors would like to acknowledge Tina Jellesmark-Jensen, Eileen McCall, Josefine Claesson, Thomas Falkamn and Mats Ormö for the preparation of human XO protein. The authors are grateful to Stefan von Berg for discussions and input in this manuscript.

Supplementary data

Supplementary data associated with this article can be found, in the online version, at http://dx.doi.org/10.1016/j.bmcl.2014.01.050.

References and notes

1. Borges, F.; Fernandes, E.; Roleira, F. *Curr. Med. Chem.* **2002**, *9*, 195.
2. Pacher, P.; Nivorozhkin, A.; Szab, C. *Pharmacol. Rev.* **2006**, *58*, 87.
3. Harrison, R. *Drug Metab. Rev.* **2004**, *36*, 363.
4. Bouez, A.; Damarla, M.; Hassoun, P. M. A. *Am. J. Physiol. Lung Cell. Mol. Physiol.* **2008**, *294*, 830.
5. Kim, B. S.; Serebreni, L.; Hamdan, O.; Lan Wang, L.; Parniani, A.; Sussan, T.; Stephens, R. S.; Boyer, L.; Damarla, M.; Hassoun, P. M.; Damico, R. *Free Radical Biol. Med.* **2013**, *60*, 336.
6. (a) Massey, V.; Komani, H.; Palmer, G.; Elion, G. B. *J. Biol. Chem.* **1970**, *245*, 2837; (b) Okamoto, K.; Eger, B. T.; Nishino, T.; Pai, E. F.; Nishino, T. *Nucleosides, Nucleotides Nucleic Acids* **2008**, *27*, 888.
7. Sorbera, L. A.; Revel, L.; Rabasseda, X.; Castaner, J. *Drugs Future* **2001**, *26*, 32.
8. Ishibuchi, S.; Morimoto, H.; Oe, T.; Ikebe, T.; Inoue, H.; Fukunari, A.; Kamezawa, M.; Yamada, I.; Naka, Y. *Bioorg. Med. Chem. Lett.* **2001**, *11*, 879.
9. Matsumoto, K.; Okamoto, K.; Ashizawa, N.; Nishino, T. *J. Pharmacol. Exp. Ther.* **2011**, *336*, 95.
10. (a) B-Rao, C.; Kulkarni-Almeida, A.; Katkar, K. V.; Khanna, S.; Ghosh, U.; Keche, A.; Shah, P.; Srivastava, A.; Korde, V.; Nemmani, K. V. S.; Deshmuk, N. J.; Dixit, A.; Brahma, M. K.; Bahirat, U.; Doshi, L.; Sharma, R.; Sivaramakrishnan, H. *Bioorg. Med. Chem.* **2012**, *20*, 2930; (b) Khanna, S.; Burudkar, S.; Bajaj, K.; Shah,

P.; Keche, A.; Ghosh, U.; Desai, A.; Srivastava, A.; Kulkarni-Almeida, A.; Deshmukh, N. J.; Dixit, A.; Brahma, M. K.; Bahirat, U.; Doshi, L.; Nemmani, K. V.; Tannu, P.; Damre, A.; B-Rao, C.; Sharma, R.; Sivaramakrishnan, H. *Bioorg. Med. Chem. Lett.* **2012**, *22*, 7543; (c) Bajaj, K.; Burudkar, S.; Shah, P.; Keche, A.; Ghosh, U.; Tannu, P.; Khanna, S.; Srivastava, A.; Deshmukh, N. J.; Dixit, A.; Ahire, Y.; Damre, A.; Nemmani, K. V. S.; Kulkarni-Almeida, A.; B-Rao, C.; Sharm, R.; Sivaramakrishnan, H. *Bioorg. Med. Chem. Lett.* **2013**, *23*, 834.

11. Sathisha, K. R.; Khanum, S. A.; Chandra, J. N. N. S.; Ayisha, F.; Balaji, S.; Mrathe, G. K.; Gopal, S.; Rangappa, K. S. *Bioorg. Med. Chem. Lett.* **2012**, *22*, 7543.
12. Leigh, M.; Raines, D. J.; Castillo, C. E.; Duhme-Klair, A. K. *ChemMedChem* **2011**, *6*, 1107.
13. Hu, L.; Hu, H.; Wu, W.; Chai, X.; Luo, J.; Wu, Q. *Bioorg. Med. Chem. Lett.* **2011**, *21*, 4013.
14. Nepali, K.; Agarwal, A.; Sapra, S.; Mittal, V.; Kumar, R.; Banerjee, U. C.; Gupta, M. K.; Satti, N. K.; Suri, O. P.; Dhar, K. L. *Bioorg. Med. Chem. Lett.* **2011**, *19*, 5569.
15. Bovine XO, purchased either from Sigma (X-4500) or CalBio (#682151), was used for the HTS and NMR assay. For HTS bXO was diluted directly into the assay buffer. For the NMR studies bXO was purified using size exclusion chromatography prior to use. Experiments were conducted in 50 mM deuterated Tris–HCl buffer at pH 7.5. For subsequent IC_{50} determinations C-terminally FLAG tagged human Xanthine Oxidase (aa 1–1333) was used. hXO was overexpressed using the Bac-to-Bac Baculo Virus expression system in High Five cells (Life Technologies) and purified by a combination of FLAG gel capture and size exclusion chromatography into the buffer 50 mM Tris–HCl pH 7.6, 0.1 M NaCl. To a 384 well plate, containing a solution of human XO (9.5 μL, 105 nmol in 0.1 M Tris–HCl, pH 7.5), were added test compounds (0.5 μL, 10 mM in DMSO) at different concentrations. After incubation at rt for 15 min, 10 μL of a solution of Xanthine (200 μM in 0.1 M Tris HCl, pH 7.5) was added. The reaction was allowed to run for 60 min at RT, then Quantichrom reagent (20 μL, BioAssay Systems, USA: http://www.bioassaysys.com/file_dir/DIUA.pdf) was added and the plate incubated for 30 min. The absorbance was measured at 590 nm using a SpectraMax 384 reader.
16. Sink, R.; Gobec, S.; Pecar, S.; Zega, A. *Curr. Med. Chem.* **2010**, *17*, 4231.
17. (a) Hajduk, P. J.; Olejniczak, E. T.; Fesik, S. W. *J. Am. Chem. Soc.* **1996**, *119*, 12257; (b) Dalvit, C.; Flocco, M.; Knapp, S.; Mostardini, M.; Perego, R.; Stockman, B. J.; Veronesi, M.; Varasi, M. *J. Am. Chem. Soc.* **2002**, *124*, 7002; (c) Jahnke, W.; Floersheim, P.; Ostermeier, C.; Zhang, X.; Hemmig, R.; Hurth, K.; Uzunov, D. *Angew. Chem., Int. Ed.* **2002**, *41*, 3420.
18. Enroth, C.; Eger, B. T.; Okamoto, K.; Nishino, T.; Nishino, T.; Pai, E. F. *Proc. Natl. Acad. Sci. U.S.A.* **2000**, *97*, 10723.
19. (a) Shultz, M. D. *Bioorg. Med. Chem. Lett.* **2013**, *23*, 5992; (b) Perola, E. *J. Med. Chem.* **2010**, *53*, 2986; (c) Leeson, P. D.; Springthorpe, B. *Nat. Rev. Drug Disc.* **2007**, *6*, 881.
20. The optimization of **4** will be published in due course.
21. (a) Okamoto, K.; Eger, B. T.; Nishino, T.; Kondo, S.; Pai, E. F.; Nishino, T. *J. Biol. Chem.* **2003**, *278*, 1848; b) Details on model construction, docking and coordinates of selected molecules can be found in the supplementary material.
22. SAR from the Rao group[10c] shows that for R^3 = H, such as compound **18**, removal of the carbonyl in the 4-position or the amino group in the 2-position leads to a 3–4-fold loss in potency.
23. McGinnity, D. F.; Parker, A. J.; Soars, M.; Riley, R. J. *Drug Metab. Dispos.* **2000**, *28*, 1327.
24. Nguyen, M. T.; Awale, S. *Biol. Pharm. Bull.* **2005**, 2231.
25. Arturson, P.; Karlsson, J. *Biochem. Biophys. Res. Commun.* **1991**, *175*, 880.
26. Compounds were tested in male Sprague Dawley rats (obtained from Charles River Laboratories, UK) for their ability to decrease hyperuricemia caused by potassium oxonate. Hyperuricemia was induced in the animals one hour before compound treatment by ip dosing of a volume of 5 mL/kg of a 60 mg/mL potassium oxonate solution in 0.9% saline. Test compounds or vehicle were given p.o. once in a volume of 10 mL/kg. Each test group contained 5 animals. At the indicated time points, blood samples were collected from the tongue vein and the levels of uric acid and test compounds were determined.
27. (a) Skulnick, H. I.; Ludens, J. H.; Wendling, M. G.; Glenn, E. M.; Rohloff, N. A.; Smith, R. J.; Wierenga, W. *J. Med. Chem.* **1986**, *29*, 1499; (b) Skulnick, H. I.; Weed, S. D.; Eidson, E. E.; Renis, H. E.; Stringfellow, D. A.; Wierenga, W. *J. Med. Chem.* **1985**, *28*, 1846.
28. Bararjanian, M.; Balalaie, S.; Barouti, S.; Rominger, F. *Helv. Chim. Acta* **2010**, *93*, 777.
29. Hannah, D. R.; Sherer, E. C.; Davies, R. V.; Titman, R. B.; Laughton, C. A.; Stevens, M. F. G. *Bioorg. Med. Chem.* **2000**, *8*, 739.